J Appl Physiol 121: 589–591, 2016;
doi:10.1152/japplphysiol.01049.2015.

VIEWPOINT

Could lobar flow sequencing account for convection-dependent ventilation heterogeneity in normal humans?

Sylvia Verbanck[1] and Manuel Paiva[2]

[1]*Respiratory Division, University Hospital UZ Brussel, Brussels, Belgium; and* [2]*Respiratory Division, University Hospital Erasme, Université Libre de Bruxelles, Brussels, Belgium*

INDICES OF CONVECTION-DEPENDENT ventilation heterogeneity have been used as a means to noninvasively sample airway structure down to the entrance of the gas exchanging zone. Although potentially attractive to reflect abnormal function of small nonalveolated airways or entire tissue units as small as acini, these indices can also be affected by much larger-scale ventilation heterogeneity. For instance in normal humans, gravity causes greater specific ventilation in the dependent parts of the lungs in the line of gravity (6, 12). Irrespective of the scale at which it is generated, convection-dependent concentration heterogeneity produces a curvilinear washout at the mouth, i.e., a curvilinear semilog plot of breath-by-breath mean expired concentration of a multiple breath washout (MBW) (22). This can be quantified by a nonzero Curv (23), with a maximum value of 1, which corresponds to the presence of an infinitesimally slow lung unit. If in addition to a nonzero Curv, the best ventilated lung units are the ones to contribute relatively more to expiratory flow in the early vs. late phase of each expiration, this produces a positive N_2 phase III slope that shows a breath-by-breath increase when normalized by expired concentration (2); this increase is most often characterized by the index Scond (18, 23). It follows that a nonzero Scond always implies that Curv is nonzero too, although a nonzero Curv can be associated with zero Scond (in the absence of flow sequencing, i.e., all flow proportions constant during expiration). MBW experiments in microgravity and in different body postures (16, 17, 19) can lead to different Curv and Scond values, but in normal humans both indices are nonzero and Scond (and the underlying N_2 phase III slope) is always positive.

Address for reprint requests and other correspondence: S. Verbanck, Respiratory Division, Univ. Hospital UZ Brussel, Laarbeeklaan 101, 1090 Brussels, Belgium (e-mail: sylvia.verbanck@uzbrussel.be).

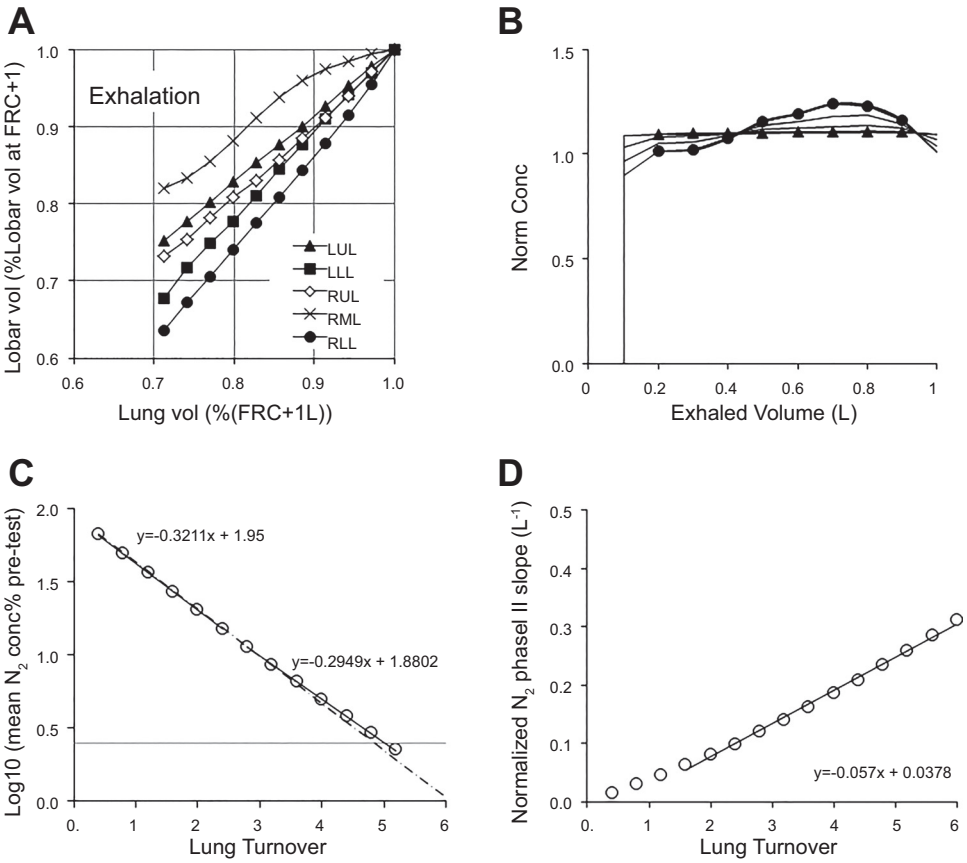

Fig. 1. *A*: expiratory lobar volume vs. total lung volume, as a percentage of respective end-inspiratory volumes, for the 5 lobes according to the digitization of Fig. 5 in Jahani et al. (8) (considering respiration between FRC and FRC+1l). *B*: N_2 concentration traces for breath number 1, 5, 10, and 15 (normalized to mean expired N_2 concentration over the entire breath including dead space), resulting from each subsequent O_2 inspiration according to the lobar volume distribution in *A* (considering 5 lobar compartments, FRC = 2.5 liters and 100 ml dead space). ▲ (breath 1) and ● (breath 15) show the concentrations that were used for calculation of phase III slope regression within each expiration. *C* and *D*: washout simulations of N_2 gas concentration and normalized N_2 phase III slopes vs. lung turnover, resulting from each subsequent O_2 inspiration according to the lobar volume distribution in *A* (considering 5 lobar compartments, FRC = 2.5 liters and 100 ml dead space); uniform mixing is also represented (dashed dotted line). The corresponding simulated Curv = 0.08 (= 1-0.2949/0.3211; one minus the regression slope ratio over the 2 halves of the turnover range down to 1/40th initial concentration in the washout concentration curve indicated by the grey horizontal line) and simulated Scond = 0.057 liter^{-1} (regression slope of normalized N_2 phase III slope between 1.5 and 6 lung turnovers).

Based on data obtained from radiopaque parenchymal markers in dog lungs (7, 14), Wilson et al. (27) suggested that the N_2 phase III slope observed in excised dog lobes could be due to increased ventilation variability at a small (intraregional) scale. At least two intraregional mechanisms, parenchymal expansion dynamics (26) and airway-parenchyma interdependence (10), have the potential to generate both conditions for a nonzero phase III slope: specific ventilation heterogeneity and expiratory flow sequencing. Thus far it has been impossible to demonstrate that either mechanism alone or embedded in a realistic airway network (13) would automatically, and without any parameter fitting, lead to a positive simulated N_2 phase III slope in normal humans. When Young and Martin investigated the role of lobar dynamics on ventilation heterogeneity by means of challenging bronchoscopic experiments (9, 11, 28), they reported flow or concentration measurements between lobes in a single lung to specifically assess upper and lower lung zones (9) or to infer that interlobar effects on concentration traces are overridden by intralobar effects (28). In the meantime, these intralobar effects can be accounted for in large part by diffusion-convection-dependent ventilation heterogeneity (15). Modeling and experimental studies (15, 25) have shown why diffusion-convection interaction in the lung periphery always generates a positive N_2 phase III slope. As for the intraregional convection-dependent part of the N_2 phase III slope in normal humans that was already the subject of a literature study 30 years ago (4), the jury is still out. Based on recent lung imaging data, the present Viewpoint explores the possibility that the interplay between all five lung lobes could in fact produce a positive N_2 phase III slope and therefore at least partly account for Scond in normal humans.

A dynamic CT study on 6 healthy subjects aged 24-58 years (8) measured lobar volumes at 20 intervals within tidal breathing cycles. In Fig. 1, we plotted these lobar volumes vs. total lung volume, resembling the familiar onion skin diagram (12), but adapted to a 1-liter volume excursion starting from FRC (and showing only the expiratory volume excursions) (Fig. 1*A*). This shows that with the subjects supine in the CT, the diaphragmatic lobes are still the ones being least expanded at FRC and best ventilated. This alone will generate a nonzero Curv. In addition, the curvilinear plots in Fig. 1*A* signal flow sequencing that can also generate a nonzero Scond. Both Curv and Scond can be simulated as follows. Using Fig. 1*A*, end-inspiratory concentrations in each lobe can be computed and recombined according to expiratory flows from each lobe to simulate a washout curve (23) (Fig. 1, *B–D*); this obtains Curv = 0.08 and Scond = 0.057 liter^{-1}. By comparing these simulated values to average experimental data for a 40-yr-old normal subject (Curv = 0.18 and Scond = 0.032 liter^{-1}) (24), we observe that specific ventilation heterogeneity (affecting Curv and Scond) is too small and flow sequencing (affecting only Scond) is too big to match normal conductive ventilation heterogeneity. Calculations would need to be repeated on per-subject sets of dynamic lobar flow curves to also assess intersubject variability. Nevertheless, the importance of this small lobar data set (8) is that it reveals a pattern of lobar flow sequencing that is compatible with a nonzero, and indeed positive, N_2 phase III slope.

In a larger group of almost 100 normal never-smoker subjects aged 45–80 yr lobar volumes at FRC and near TLC were obtained by static CT (29). If in a first approximation, we assume that relative lobar volume changes between FRC and FRC+1l are proportional to those between FRC and TLC, this results in simulated Curv = 0.19 (male) and 0.25 (female) [average experimental Curv = 0.24 for a 60-yr-old normal subject (24)]. Depending on the degree of nonlinearity in lobar volume excursions between FRC and TLC, the estimate of Curv will be affected. However, dynamic CT studies measuring such nonlinearity (8) cannot be readily reproduced in a large healthy population for ethical reasons. Ventilation modalities that visualize inhaled tracer concentration by scintigraphy (5) or MRI (1) would also require a delineation of lobes, for instance by registration with CT images at some instances in the breathing cycle. Still, this might not obtain the appropriate accuracy to distinguish a real difference in relative lobar specific ventilation from its measurement noise; the latter would also lead to a simulated nonzero Curv. An attractive alternative is the measurement of velocity profiles over the cross sections of the main bronchi by MRI phase-contrast velocimetry (1), which has been able to show that at very low flows and in the supine position, there is a cardiogenic pendelluft between the left and right lung lobes (1, 21). Despite considerable intersubject variability, the lobar expansion and deflation was seen to be most frequently influenced by local volume changes in synchrony with the heart beat in the left lower lobe (1). Potentially, this technique could be elaborated further to also obtain velocity over the five bronchi leading to the five lobes and derive lobar flows during a full breathing cycle.

We conclude this Viewpoint by contending that lobar expansion is a likely contributor to the convection-dependent N_2 phase III slope and that an adaptation of noninvasive imaging (1) or reanalysis of existing CT data (8) could help confirm or refute this hypothesis. Because the recumbent body posture during imaging likely affects functional residual capacity (3) and lobar expansion, these imaging data strictly apply only to MBW tests performed in the same posture. A bronchoscopic system currently used to detect collateral ventilation in chronic obstructive lung patients eligible for lobar resection (20) could be modified to obtain relative lobar flows in upright humans, provided flow cycles measured in the five different lobar bronchi can be properly aligned to quantify flow sequencing between them.

DISCLOSURES

No conflicts of interest, financial or otherwise, are declared by the author(s).

AUTHOR CONTRIBUTIONS

S.A.V. drafted manuscript; S.A.V. and M.P. edited and revised manuscript; S.A.V. and M.P. approved final version of manuscript.

REFERENCES

1. **Collier GJ, Marshall H, Rao M, Stewart NJ, Capener D, Wild JM.** Observation of cardiogenic flow oscillations in healthy subjects with hyperpolarized 3He MRI. *J Appl Physiol* 119: 1007–1014, 2015.
2. **Crawford ABH, Makowska M, Paiva M, Engel LA.** Convection- and diffusion-dependent ventilation maldistribution in normal subjects. *J Appl Physiol* 59: 838–846, 1985.
3. **Elliott AR, Prisk GK, Guy HJ, West JB.** Lung volumes during sustained microgravity on Spacelab SLS-1. *J Appl Physiol* 77: 2005–2014, 1994.
4. **Engel LA.** Intraregional gas mixing and distribution. In: *Gas Mixing and Distribution in the Lung*, edited by Engel LA and Paiva M. New York: Marcel Dekker, 1985, p. 287–358.

5. **Farrow CE, Salome CM, Harris BE, Bailey DL, Bailey E, Berend N, Young IH, King GG.** Airway closure on imaging relates to airway hyperresponsiveness and peripheral airway disease in asthma. *J Appl Physiol* 113: 958–966, 2012.
6. **Guy HJ, Prisk GK, Elliott AR, Deutschman RA 3rd, West JB.** Inhomogeneity of pulmonary ventilation during sustained microgravity as determined by single-breath washouts. *J Appl Physiol* 76: 1719–1729, 1994.
7. **Hubmayr RD, Walters BJ, Chevalier PA, Rodarte JR, Olson LE.** Topographical distribution of regional lung volume in anesthetized dogs. *J Appl Physiol Respir Environ Exercise Physiol* 54: 1048-1045, 1983.
8. **Jahani N, Choi S, Choi J, Iyer K, Hoffman EA, Lin CL.** Assessment of regional ventilation and deformation using 4D-CT imaging for healthy human lungs during tidal breathing. *J Appl Physiol* 119: 1064–1074, 2015.
9. **Koler JJ, Young AC, Martin CJ.** Relative volume changes between lobes of the lung. *J Appl Physiol* 14: 345–347, 1959.
10. **Ma B, Bates JH.** Mechanical interactions between adjacent airways in the lung. *J Appl Physiol* 116: 628–634, 2014.
11. **Martin CJ, Young AC.** Lobar ventilation in man. *Am Rev Tuberc* 73: 330–337, 1956.
12. **Milic-Emili J, Henderson JAM, Dolovich MB, Trop D, Kaneko K.** Regional distribution of inspired gas in the lung. *J Appl Physiol* 21: 749–759, 1966.
13. **Mitchell JH, Hoffman EA, Tawhai MH.** Relating indices of inert gas washout to localised bronchoconstriction. *Respir Physiol Neurobiol* 183: 224–233, 2012.
14. **Olson LE, Rodarte JR.** Regional differences in expansion in excised dog lung lobes. *J Appl Physiol Respir Environ Exercise Physiol* 57: 1710–1714, 1984.
15. **Paiva M, Engel LA.** Gas mixing in the lung periphery. In: *Respiratory Physiology*, edited by Chang HK and Paiva M. New York: Dekker, 1989, vol. 40, p. 245–276.
16. **Prisk GK, Elliott AR, Guy HJ, Verbanck S, Paiva M, West JB.** Multiple-breath washin of helium and sulfur hexafluoride in sustained microgravity. *J Appl Physiol* 84: 244–252, 1998.
17. **Prisk GK, Guy HJ, Elliott AR, Paiva M, West JB.** Ventilatory inhomogeneity determined from multiple-breath washouts during sustained microgravity on Spacelab SLS-1. *J Appl Physiol* 78: 597–607, 1995.
18. **Robinson PD, Latzin P, Verbanck S, Hall GL, Horsley A, Gappa M, Thamrin C, Arets HG, Aurora P, Fuchs SI, King GG, Lum S, Macleod K, Paiva M, Pillow JJ, Ranganathan S, Ratjen F, Singer F, Sonnappa S, Stocks J, Subbarao P, Thompson BR, Gustafsson PM.** Consensus statement for inert gas washout measurement using multiple- and single-breath tests. *Eur Respir J* 41: 507–522, 2013.
19. **Rodríguez-Nieto MJ, Peces-Barba G, González Mangado N, Paiva M, Verbanck S.** Similar ventilation distribution in normal subjects prone and supine during tidal breathing. *J Appl Physiol* 92: 622–626, 2002.
20. **Shah PL, Herth FJ.** Dynamic expiratory airway collapse and evaluation of collateral ventilation with Chartis. *Thorax* 69: 290–291, 2014.
21. **Sun Y, Butler JP, Ferrigno M, Albert MS, Loring SH.** "Ventilatory alternans": a left-right alternation of inspiratory airflow in humans. *Respir Physiol Neurobiol* 185: 468–471, 2013.
22. **Verbanck S, Paiva M.** Gas mixing in the airways and airspaces. *Compr Physiol* 1: 809–834, 2011.
23. **Verbanck S, Paiva M, Schuermans D, Malfroot A, Vincken W, Vanderhelst E.** Acinar and conductive ventilation heterogeneity in severe CF lung disease: back to the model. *Respir Physiol Neurobiol* 188: 124–132, 2013.
24. **Verbanck S, Van Muylem A, Schuermans D, Bautmans I, Thompson B, Vincken W.** Transfer factor, lung volumes, resistance and ventilation distribution in healthy adults. *Eur Respir J* 47: 166–176, 2016.
25. **Verbanck S, Weibel ER, Paiva M.** Simulations of washout experiments in postmortem rat lungs. *J Appl Physiol* 75: 441–451, 1993.
26. **Wilson TA.** Parenchymal mechanics, gas mixing, and the slope of phase III. *J Appl Physiol* 115: 64–70, 2013.
27. **Wilson TA, Olson LE, Rodarte JR.** Effect of variable parenchymal expansion on gas mixing. *J Appl Physiol* 62: 634–639, 1987.
28. **Young AC, Martin CJ.** The sequence of lobar emptying in man. *Respir Physiol* 1: 372–381, 1966.
29. **Zach JA, Newell JD Jr, Schroeder J, Murphy JR, Curran-Everett D, Hoffman EA, Westgate PM, Han MK, Silverman EK, Crapo JD, Lynch DA; COPDGene Investigators.** Quantitative computed tomography of the lungs and airways in healthy nonsmoking adults. *Invest Radiol* 47: 596–602, 2012.